

Fire Detection in the Urban Rural Interface through Fusion techniques

E. Zervas
Dept. of Electronics
TEI-Athens
12210 Athens, Greece
Email: zervas@ee.teiath.gr

O. Sekkas, S. Hadjieftymiades, C. Anagnostopoulos
Dept. of Informatics and Telecommunications
University of Athens
15784 Athens, Greece
Email: {sekkas,shadj, bleu}@di.uoa.gr

Abstract

Fires are a common, disastrous phenomenon that constitutes a serious threat. Thus, early detection is of great importance as the consequences of a fire are catastrophic. Towards this direction the SCIER¹ project envisages the deployment of Wireless Sensor Networks at the “Urban-Rural-Interface” (URI) and uses sensor fusion techniques to enhance the performance of the early fire detection and fire location estimation processes.

1 Introduction

Fires are a common, disastrous phenomenon that constitutes a serious threat. Because of their speed of spread and intensity they often lead to property damages, personal injuries and loss of human lives. Thus, early detection is of great importance as the consequences of a fire (indoor or outdoor) are catastrophic. Fires that occur in wildland (forests, etc.) could also affect inhabited areas. These areas are widely known as “Urban-Rural-Interface” (URI), i.e., zones where forests and rural lands interface with homes, other buildings and infrastructures. In the URI, fires are frequent due to the special nature of these zones; a fire could be the result either of human on one side of the zone, or could arrive from the other side (wildland). In such cases early detection leads to an efficient control of the fire and makes feasible the immediate evacuation of the entire area if this is considered necessary. Great technology effort has been invested on the design of systems for fire detection and monitoring. Most of them make use of temperature and humidity sensors, smoke detectors, infrared cameras, etc. In addition, aerial or satellite images are frequently used for outdoor fire detection and monitoring. In [3] a fire detection system is

proposed based on multi-sensor technology and neural networks (NNs). The sensed data include environmental temperature, smoke density and CO density. The use of NNs for automatic detection of smoke is also proposed in [10]. A system for wildfire monitoring using a wireless sensor network (WSN) that collects temperature relative humidity and barometric pressure is described in [4]. The wireless networked nodes communicate with a base station that collects the sensed data. Satellite based monitoring [11] is another method to detect forest fires but the scan period and the low resolution of satellite images make this method incapable for real-time detection. The authors in [2] and [7] propose systems based on infrared (IR) technology for the detection of fires.

The SCIER project will design, develop, and demonstrate an integrated system of sensors, networking and computing infrastructure for detecting, monitoring and predicting natural hazards (fires, etc.) at the URI. The overall goal of the SCIER system is to make the neglected URI zone safer against any type of natural hazards or accidents using wireless sensor network technologies, fusion techniques to assess dangerous situations, and predictive models to estimate the evolution of the hazardous phenomena. The fusion techniques used in SCIER are implemented in a special component of the SCIER system: the Local Alerting Control Unit (LACU). LACU controls a Wireless Sensor Network (WSN) and is responsible for the early detection of potential fires, the fire location estimation and the subsequent alerting functions. For the detection phase, sensor readings are evaluated and probabilities are assigned on each situation. If the probability of fire event exceeds a predetermined threshold, the system shifts to fire location estimation phase. In this phase the centre of the fire outbreak and the radius of the fire spread are determined.

The rest of the paper is organized as follows: in Section 2 the SCIER architecture is described and the requirements concerning the topology of the wireless sensors controlled by LACU are defined. Section 3 discusses fire detection and fire location estimation based on sensor readings (temperature) and sensor location (GPS coordinates). Finally in

¹SCIER (Sensor & Computing Infrastructure for Environmental Risks) is partially funded by the European Community through the FP6 IST Program. The work presented in this paper expresses the ideas of the authors and not necessarily the whole SCIER consortium.

Section 4 conclusions are presented and open research issues are discussed.

2 System Architecture - Requirements

The SCIER system constitutes an integrated platform of sensors and computing infrastructure capable of delivering valuable real time information regarding natural hazards at the “Urban-Rural-Interface” (Fig. 1). As an environmental hazard approaches, or has occurred in the URI region, SCIER will provide the capabilities of both monitoring and predicting its evolution. Sensors spread in the region will monitor environmental parameters (e.g., temperature) and feed with already fused data the predictive models in the computing infrastructure. SCIER system is composed by three entities: the Sensing Subsystem, the Computing Subsystem and the Localized Alerting Subsystem.

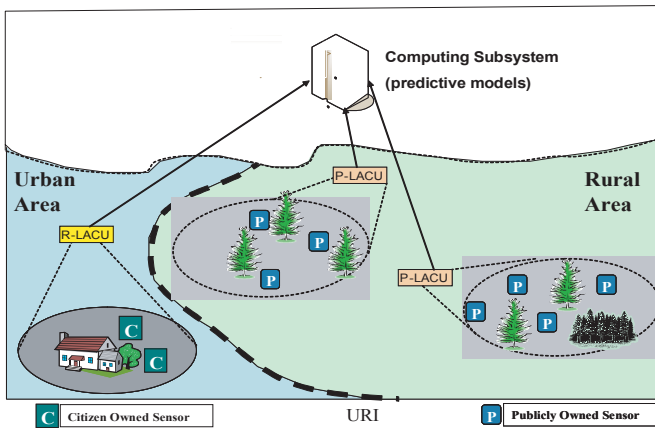


Figure 1. SCIER system at the URI.

2.1 The Sensing Subsystem

In URI two kind of sensors are deployed: Citizen Owned Sensors (COS), installed by land/home owners in fixed and registered locations in private areas, and Publicly Owned Sensors (POS), installed by state authorities in fixed and known locations in public areas. In SCIER system the use of temperature, humidity and air direction/speed sensors is adopted.

2.2 The Computing Subsystem

This subsystem is based on GIS (e.g., region, URI) where the fused sensor information is fed. Multiple mathematical environmental models of different time scales are used in order to establish a highly accurate tracking of the hazardous phenomenon. The output of the models will, in certain cases, re-feed the sensor infrastructure, which will be capable of reconfiguring itself to adapt to the dynamics of the observed phenomenon and allow its best monitoring.

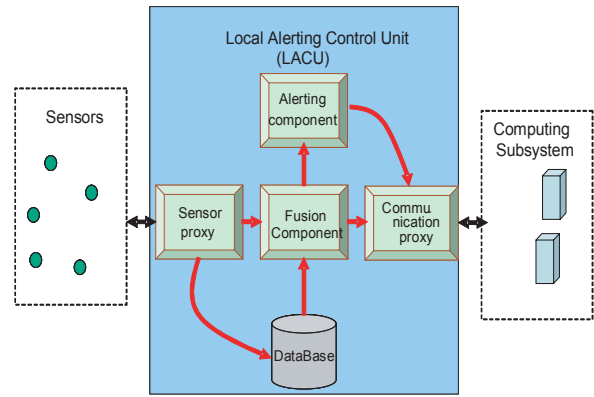


Figure 2. LACU architecture.

2.3 The Localized Alerting Subsystem (LAS)

LAS includes the Local Alerting Control Unit (LACU) which controls an area of deployed sensors and performs fusion algorithms for fire detection and fire location estimation. In SCIER, two types of LACUs are identified (Fig. 1):

- **Public LACU (P-LACU).** This type of LACU is installed and operated by public authorities and controls a wireless network of Public Owned Sensors.
- **Private LACU (R-LACU).** This type of LACU controls Citizen Owned Sensors and is installed by individuals in order to protect their private properties.

LACU is a device which resides between the Computing Subsystem and the Sensing Subsystem as depicted in Fig. 2. The basic components that comprise LACU and their role are described in the following paragraphs.

- **Communication proxy**, which is responsible for the communication between LACU and Computing Subsystem.
- **Sensor proxy**, which receives and stores readings transmitted by the sensors deployed in the monitored area.
- **Fusion component**, which assesses sensor data and determines if a fire outbreak occurs in the area. Furthermore, it estimates the exact location of the fire.
- **Alerting component**, which is triggered by Fusion Component and provides notifications to the Computing Subsystem and to the users (in case of an R-LACU) when an emergency situation occurs (e.g fire).
- **Data Base**, which stores historical data, the identification of each sensor and its location as well as the readings arriving from the Sensor proxy.

The topology of the WSN controlled by a LACU (public or private) plays an important role in the fusion process. The

density of sensors depends on the area that is monitored and the desired accuracy of fire location estimation. For the fire detection process an issue arises regarding the false alarm rate of the system. A false alarm is the situation when the detection algorithm decides that there is a fire and actually there is not. It is clear that if we need a reasonable number of false alarms then the detection latency of the system increases (i.e. it is possible to not detect a fire). The false alarm rate is parameterized and it depends on the user requirements (in case of an R-LACU), on season of the year (e.g. summer) and on the risk factor of the monitored area.

3 Fire detection and Fire Location Estimation

The two problems of fire detection and fire location estimation are treated separately. Temperature sensors, scattered at the LACU area, continuously monitor the environment for abrupt temperature changes. Upon a fire event detection, the sensors continue to send their readings at the LACU where a fire location estimation process follows.

3.1 Fire detection

Several sequential detection techniques have been proposed in the literature including Bayesian formulations [8] and the CUSUM procedure[6]. In this paper we follow a simple approach formulating detection as a binary hypothesis problem and using the Maximum Likelihood (ML) criterion to decide upon the two events: No Fire (Hypothesis 0) and Fire (Hypothesis 1). That is,

$$\hat{j} = \arg \max_{j \in \{0,1\}} p_j(\mathbf{z}) \quad (1)$$

where \mathbf{z} is the set of measurements and $p_j(\mathbf{z})$ is the p.d.f. of the measurements under hypothesis j . We assume that $p_j(\mathbf{z})$ follows a Gaussian distribution

$$p_j(\mathbf{z}) \sim \mathcal{N}(\mathbf{m}_j, \Sigma_j)$$

and we attempt to model the parameters \mathbf{m}_j and Σ_j

Let us consider K sensors placed ad hoc in the LACU area, as shown in Fig. 3, and let R_j denote the radius of a disk with center the sensor j . Assuming disks of equal radius ($R_j = r$), we can find the minimum value of r , such that a full coverage of the LACU area is obtained, that is

$$R = \min r, \quad \text{s.t.c. } \cup_j r \subset \mathcal{L}$$

where \mathcal{L} is the LACU area. This calculation is possible since the position of the sensors is known beforehand at the LACU. The value of R is critical regarding the redundancy of the measurements and the detection latency. In the absence of a fire event the measurements of sensor j are modeled as

$$z_j = s_j + n_j \quad (2)$$

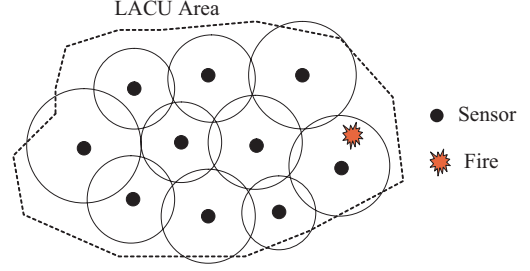


Figure 3. Temperature sensors in the LACU area.

where n_j is the sensor measurement noise, assumed to be Gaussian with zero mean and variance σ_n^2 which is provided by the sensor manufacturer. Next we assume that s_j is Gaussian with mean $\mu(h)$ and variance σ_s^2 , that is

$$s_j \sim \mathcal{N}(\mu(h), \sigma_s^2) \quad (3)$$

The mean $\mu(h)$ depends on the **hour** of the date and the **month** of the year and can be estimated from statistical data (stored in the database of LACU), empirical models, forecasting, or even the sensors themselves. Thus, $\mu(h)$ can be obtained by a weighted average of all aforementioned estimation techniques, such as

$$\begin{aligned} \mu(h) &= w_1 \mu^e(h) + w_2 \mu^h(h) + w_3 \mu^f(h) + w_4 \mu^m(h) \\ \sum_i w_i &= 1, \quad w_4 > w_3 > w_2 > w_1 \end{aligned}$$

where the superscripts e, h, f and m denote empirical, historical, forecasting and measured estimates respectively. For example, Walters' model ([9]) provides the "average unit curve" given by

$$\begin{aligned} X_a(h) &= 0.463 \sin(B + 232^\circ 38') + 0.121 \sin(2B + 55^\circ 21') \\ &\quad + 0.031 \sin(3B + 73^\circ 19') \end{aligned}$$

where $X_a(h)$ is the unit ordinate at time h (Local Apparent Time, LAT), B is angular measure of the time of day, h (LAT), $0 < B < 360^\circ$, $B = 15h$. Using this formula along with

$$X_a(h) = \frac{\mu^e(h) - T_m}{T_{\max} - T_{\min}}$$

we can estimate the screen temperature $\mu^e(h)$ at time h . T_{\max} is the maximum temperature, T_{\min} is the minimum temperature of the day and T_m is the mean of the 24 hourly temperatures. For these parameters we can use statistical data or the previous day values. For example if $T_{max} = 35C^\circ$, $T_{min} = 12C^\circ$ and $T_m = 20C^\circ$ we obtain the daily variations of temperature of Fig. 4, which shows that temperature is higher at 2:00-3:00 pm. For the estimation of $\mu^m(h)$ by the sensors themselves, we drop the D highest

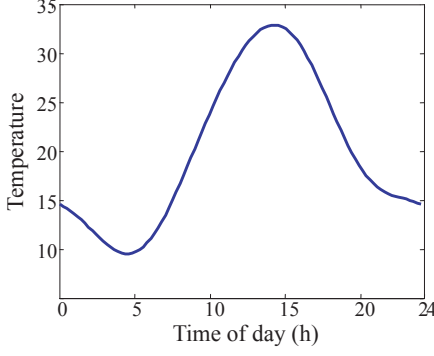


Figure 4. Empirical estimation of $\mu(h)$

and lowest temperature measurements out of the K available and we estimate $\mu^m(h)$ by

$$\mu^m(h) = \frac{1}{K-2D} \sum_{j=D+1}^{K-D} \tilde{z}_j$$

where \tilde{z}_j are the ordered (in increasing value) temperature measurements. This averaging can be considered as a simple data fusion process.

The parameter σ_s in (3), controls the variations (i.e. clouds, rainy day) from the mean value $\mu(h)$. Next suppose that we have K measurements $\{z_1, z_2, \dots, z_K\}$ from different nodes available to us. Consider the K -dimensional vector

$$\mathbf{z} = [z_1, z_2, \dots, z_K]^T$$

Under Hypothesis 0 (no fire event) this vector is Gaussian distributed with mean $\mathbf{m}_0 = [\mu(h), \dots, \mu(h)]^T$ and covariance matrix Σ_0 . The covariance matrix has the form

$$\Sigma_0 = \begin{pmatrix} \sigma_s^2 + \sigma_n^2 & \rho_{12}\sigma_s^2 & \dots & \rho_{1K}\sigma_s^2 \\ \rho_{21}\sigma_s^2 & \sigma_s^2 + \sigma_n^2 & \dots & \rho_{2K}\sigma_s^2 \\ \vdots & \vdots & \ddots & \vdots \\ \rho_{K1}\sigma_s^2 & \rho_{K2}\sigma_s^2 & \dots & \sigma_s^2 + \sigma_n^2 \end{pmatrix}$$

It should be noted that in the absence of fire the sensor measurements are highly correlated especially for the nearby sensors. That is the values ρ_{ij} should be close to 1. We can associate correlation coefficients based on the distance of two sensors, or even estimate the matrix Σ_0 from the sensor measurements through the formula

$$\hat{\Sigma}_0 = \frac{1}{N} \sum_{n=1}^N (\mathbf{z}_n - \mathbf{m}_0)(\mathbf{z}_n - \mathbf{m}_0)^T$$

Next we model the mean and the variance of the Gaussian distribution of the measurements given Hypothesis 1 (Fire event). In this case the measurements of sensor j take the form

$$z_j = s_j + q_j + n_j \quad (4)$$

where s_j and n_j have been defined in the no-fire case, and the random variable q_j measures the excess temperature due to fire. This variable is modeled as Gaussian with mean $\mu_q(x)$ and variance σ_q^2 , that is

$$q_j \sim \mathcal{N}(\mu_q(x), \sigma_q^2) \quad (5)$$

It should be noted that the mean $\mu_q(x)$ is a function of the distance of the sensor from the fire front. If heat radiation is the main phenomenon, then only the sensors that are in the vicinity of the fire event will detect fire. In view of this matter we consider a heat radiation model of the form

$$\mu_q(x) = \frac{\Delta H}{(1+x)^a} \quad (6)$$

where ΔH is the excess temperature at the fire location, x is the distance of the sensor from the fire front and a an exponent which can be determined through physical laws and/or simulation. To this end we consider a fire model described by the following system of partial differential equations which is derived from the conservation of energy, balance of fuel supply and fuel reaction rate [1][5].

$$\begin{aligned} \frac{dT}{dt} &= \nabla \cdot (k\nabla T) + v \cdot \nabla T + AF e^{-B/(T-T_a)} - C(T - T_a) \\ \frac{dF}{dt} &= -C_F F e^{-B/(T-T_a)}, \quad T > T_a \end{aligned} \quad (7)$$

where T and F denote temperature and fuel mass fraction respectively, with the initial conditions $F(t_0) = 1, T(t_0) = T_0$. The diffusion term $\nabla \cdot (k\nabla T)$ models short-range heat transfer by radiation, $v \cdot \nabla T$ models heat convected by the wind, $C(T - T_a)$ is the heat lost to the atmosphere (T_a is the ambient temperature), $C_F F e^{-B/(T-T_a)}$ is the rate of fuel disappearance due to burning, whereas $AF e^{-B/(T-T_a)}$ is the rate of heat generation due to burning. Fig. 5, shows an example of the propagation combustion wave and fuel supply mass fraction under no wind conditions ($v = 0$) and $k = 2.1360 \times 10^{-1} m^2 s^{-1} K^{-3}$, $A = 1.8793 \times 10^3 K s^{-1}$, $B = 5.5849 \times 10^2 K$, $C = 9.0905 \times 10^{-2} s^{-1}$, $C_F = 1.6250 s^{-1}$, $T_a = 300 K$ and $T_0 = 800 K$. The values of A and C_F are an order of magnitude greater than those used in [5] thus resulting in an extremely fast fire spread model.

Fig. 6 shows the temperature profile after 30 seconds from fire ignition at $T_0 = 0$ for the parameters of the fire model of Fig. 5. As it is observed the fire front exhibits a steep fall from 1000 K, at position $\pm 12.5m$, down to 330 K, at $\pm 15.5m$. That is, the temperature sensors will increase their readings by $30C^\circ$ if the fire front is $3m$ away. For the extreme fire spread model considered, this distance will be covered in about $5s$ which is enough for the sensor to transmit several measurements before being burnt. For this fire spread model we can estimate the exponent a in (6) to be equal to 2.3.

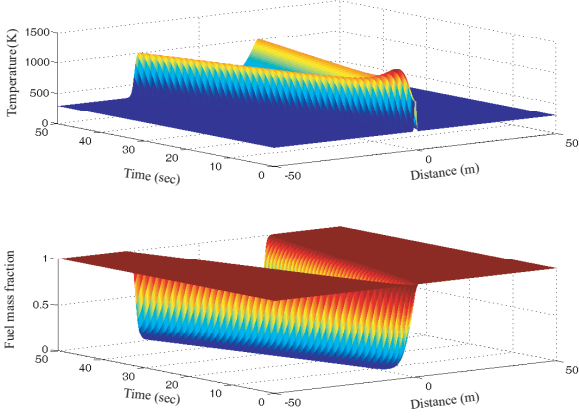


Figure 5. a) Propagating combustion wave b) Fuel supply mass fraction

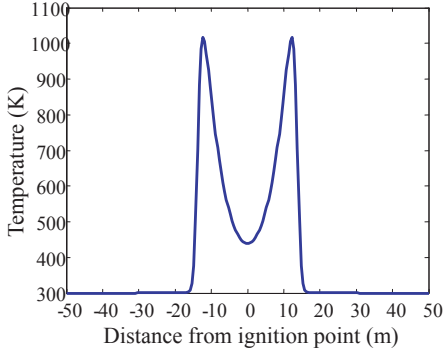


Figure 6. Temperature profile after 30s from ignition.

Since each sensor monitors an area of radius R , the distance x from the fire ignition point to the sensor is a random variable with pdf

$$f_X(x) = \frac{2x}{R^2}$$

Therefore, in view of equations (5), (6) we obtain

$$f_Q(q_j) = \int_0^R \frac{1}{\sqrt{2\pi}\sigma_q} \exp\left\{-\left(q_j - \frac{\Delta H}{(1+x)^a}\right)^2 / 2\sigma_q^2}\right\} \frac{2x}{R^2} dx$$

A simplification is obtained if we substitute $\mu_q(x)$ in (5) by its mean value

$$\begin{aligned} \mu_q &= \int_0^R \mu_q(x) f_X(x) dx \\ &= \frac{(1+R)^{(2-a)}}{2-a} - \frac{(1+R)^{(1-a)}}{1-a} + \frac{1}{(1-a)(2-a)} \end{aligned}$$

Under these conditions z_j in (4) is Gaussian distributed with mean $\mu(h) + \mu_q$ and variance $\sigma_s^2 + \sigma_q^2 + \sigma_n^2$. Due to the fact

that the number of sensors that detect fire varies (depending on fire spread and spotting), the estimation of the joint distribution of the measurement vector $\mathbf{z} = [z_1, z_2, \dots, z_K]^T$ is very complicated. Therefore, we resort to a suboptimal decision-fusion classifier where all measurements are treated as independent. For each sensor a decision is made for the existence of fire in its control territory using the ML criterion and the distributions of z_j when it takes the form in (2) and (4) respectively. ROC curves for different values of R are provided in Fig. 7. Given a desirable false alarm

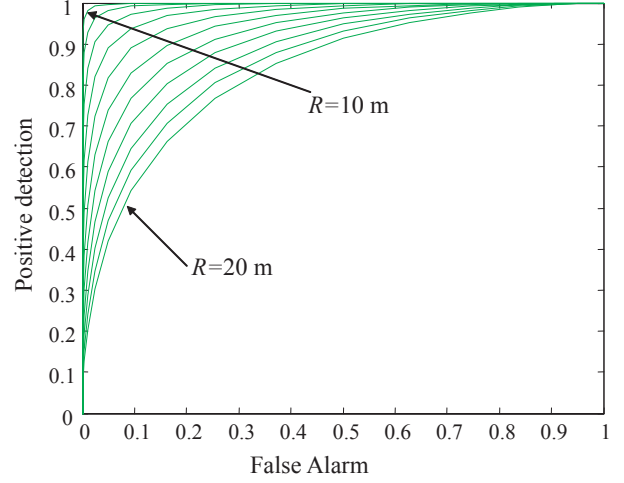


Figure 7. ROC curves ($\mu(h) = 300K$, $\sigma_s = 3$, $\sigma_n = 0.5$, $\sigma_q = 1$, $a = 2.3$, $\Delta H = 700K$).

rate and knowing the radius R for each node a threshold can be set to decide for a fire event in its territory. The detection probabilities are assessed at the LACU for the final decision fusion. This scheme enables LACU to make decisions no matter how many fire spots exist in its area. Moreover, LACU does not have to recalculate the likelihood of the vector \mathbf{z} if some of the sensors is known to be burnt or malfunctioning.

3.2 Fire location estimation

Assuming a homogeneous fuel terrain and no wind conditions the spread of fire will be circular. Moreover, if the WSN is sparse and the fire starts close to a sensor S_j then, due to the sharp leading edge of fire temperature profile, only this sensor will notice a temperature increase. Thus, at this time instant t_0 , the fire front is known at the LACU to be located in a small disk around sensor S_i . As the fire spreads, another sensor S_j will sense the temperature increase at a latter time t_1 . Needless to say that sensor S_i may be burnt by this time, but its measurements at time t_0 have been timestamped and stored at the LACU. A typical situation is depicted in Fig. 8 in case that the fire started in the convex hull of the sensors. Knowing the characteristics of the

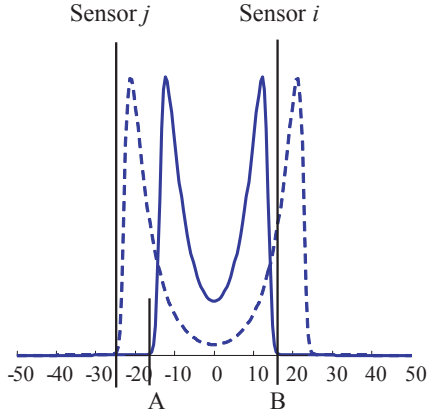


Figure 8. Combustion wave reaching two sensors.

combustion wave, i.e. speed of propagation v_f , LACU is in position to estimate the distance AB as $d_{12} - v_f(t_1 - t_0)$. Therefore the fire ignition point lies on the line normal to the midpoint of AB . A third sensor reading is needed to complete the triangularization process and find the fire starting point. Moreover, LACU is able to produce contours of fire probabilities and zones of burnt sensors which can be used to get an estimate of the fire front and the ignition point respectively. For example, if sensor nodes S_1, S_2, \dots, S_m are burnt at time instants t_1, t_2, \dots, t_m ($t_1 < t_2 < \dots < t_m$) the fire starting point is estimated via

$$(x_s, y_s) = \sum_{i=1}^m w_i(x_i, y_i), \quad \sum_i w_i = 1$$

where the weights w_i are larger for these nodes burnt earlier. On the other hand knowing the fire front at various time instants based on increased sensor measurements helps to estimate the fire spread speed and direction. Neighboring LACUs can benefit from these estimates increasing the sampling rate of their sensors and their awareness status.

4 Conclusions and Future Work

In this paper we presented the functionality of the Local Alerting Control Unit (LACU) component, as a part of the overall SCIER architecture, regarding the early detection of potential fires and the fire location estimation process. We propose a method for fire detection on an area covered by temperature sensors. Sensor readings are processed using the Maximum Likelihood (ML) criterion to decide upon the two events (Fire and No Fire). Moreover, the fire location estimation method that is proposed helps determining the fire ignition point and the fire front. Such information is obtained by fusing multiple sensor readings and knowing the location of each sensor. Knowledge of the fire front helps in adapting the data acquisition process

(e.g. increase sampling rate) and in alerting neighboring LACUs that may be affected by the fire. Currently, open research issues are investigated in the context of LACU and especially in the design and implementation of the fusion component. Besides temperature, there are also other types of sensors that can be deployed in the area and contribute to the fusion process. Humidity sensors offer an alternative way for checking and evaluating the air temperature measurements; in general air humidity declines as air temperature arises. Modelling this relationship we will be capable to confirm temperature readings, thus eliminating the probability of taking into account the data sent from a defective sensor. Furthermore, the speed and direction of the wind that flows in the monitored area and the non-homogeneous terrain affects the spread model of the fire. Incorporating such information, the fire models become more realistic and the fire detection and fire location estimation process more accurate.

References

- [1] M. I. Asensio, L. Ferragut, and J. Simon. A Convection Model for Fire Spread Simulation. *Applied Mathematics Letters, Elsevier*, 18:673–677, 2005.
- [2] A. Calle, J. L. Casanova, and A. Romo. Fire Detection and Monitoring using MSG Spinning Enhanced Visible and Infrared Imager (SEVIRI) Data. *J. Geophys. Res.*, 111, G04S06, 2006.
- [3] S. Chen, H. Bao, X. Zeng, and Y. Yang. A Fire Detecting Method based on multi-sensor Data Fusion. In *IEEE Systems Man and Cybernetics*, volume 4.
- [4] D. M. Doolin and N. Sitar. Wireless Sensors for Wildfire Monitoring. In *Smart Structures and Materials*, volume 5765, Mar. 2005.
- [5] J. M. et. al. A Wildland Fire Model with Data Assimilation. *Submitted to Elsevier*, Mar. 2007.
- [6] E. Page. Continuous Inspection Schemes. *Biometrika*, 41:100–115, 1954.
- [7] C. Sivathanu and L. K. Tseng. Fire Detection Using Near-IR Radiation and Source Temperature Discrimination. pages 117–118. National Institute of Standards and Technology. Annual Conference on Fire Research: Book of Abstracts, Oct. 1996.
- [8] V. V. Veeravalli, T. Basar, and H. V. Poor. Decentralized Sequential Detection with a Fusion Center Performing the Sequential Test. *IEEE Trans. Inform. Theory*, 39:433–442, Mar. 1993.
- [9] A. Walter. Notes on the Utilization of Records from Third Order Climatological Stations for Agricultural Purposes. *Ag. Met.*, 4:137–143, 1967.
- [10] L. Zhanqing, A. Khananian, R. Fraser, and J. Cihlar. Automatic Detection of Fire Smoke using Artificial Neural Networks and Threshold Approaches applied to AVHRR Imagery. *IEEE Trans. on Geoscience and Remote Sensing*, 39:1859–1870.
- [11] L. Zhanqing, S. Nadon, and J. Cihlar. Satellite Detection of Canadian boreal Forest Fires: development and application of the algorithm. *J. Remote Sensing*, 21:3057–3069, 2000.